NASA Technical Memorandum 100947

Oxygen Electrode Bifunctional Electrocatalyst $NiCo_2O_4$ Spinel

William L. Fielder and Joseph Singer
Lewis Research Center
Cleveland, Ohio

September 1988

NASA

Trade names or manufacturers' names are used in this report for identification only. This usage does not constitute an official endorsement, either expressed or implied, by the National Aeronautics and Space Administration.

OXYGEN ELECTRODE BIFUNCTIONAL ELECTROCATALYST $NiCo_2O_4$ SPINEL

William L. Fielder and Joseph Singer
National Aeronautics and Space Administration
Lewis Research Center
Cleveland, Ohio 44135

SUMMARY

A significant increase in energy density may be possible if a two-unit alkaline regenerative H_2-O_2 fuel cell is replaced with a single-unit system that uses passive means for H_2O transfer and thermal control. For this single-unit system, new electrocatalysts for the O_2 electrode will be required which are not only bifunctionally active but also chemically and electrochemically stable between the voltage range of about 0.7 and 1.5 V. $NiCo_2O_4$ spinel is reported to have certain characteristics that make it useful for a study of electrode fabrication techniques. High surface area $NiCo_2O_4$ powder was fabricated into unsupported, bifunctional, PTFE-bonded, porous gas fuel cell electrodes by commercial sources using varying PTFE contents and sintering temperatures. The object of the present study was to measure the bifunctional activities of these electrodes and to observe what performance differences might result from different commercial electrode fabricators.

O_2 evolution and O_2 reduction data were obtained at 80 °C (31 percent KOH). An irreversible reaction (i.e. aging) occurred during O_2 evolution at potentials greater than about 1.5 V. Anodic Tafel slopes of 0.06 and 0.12 V/decade were obtained for the aged electrodes. Within the range of 15 to 25 percent, the PTFE content was not a critical parameter for optimizing the electrode for O_2 evolution activity. Sintering temperatures between 300 and 340 °C may be adequate but heating at 275 °C may not be sufficient to properly sinter the PTFE-$NiCo_2O_4$ mixture.

Electrode disintegration was observed during O_2 reduction. Transport of O_2 to the $NiCo_2O_4$ surface became prohibitive at greater than about -0.02 A/cm^2. Cathodic Tafel slopes of -0.06 and -0.12 V/decade were assumed for the O_2 reduction process. A PTFE content of 25 percent (or greater) appears to be preferable for sintering the PTFE-$NiCo_2O_4$ mixture.

INTRODUCTION

An effective and efficient electrical power system is a major requirement for most NASA missions. One system of interest is an energy storage device in conjunction with a photovoltaic array. Desired characteristics for the storage device are light weight, low volume, high efficiency, long life and reliability. The two-unit alkaline regenerative H_2-O_2 fuel cell is one of the candidates for use in the low earth orbit (LEO) manned space station. For example, a H_2-O_2 fuel cell may be used to generate power during the dark portion of the orbit and an electrolyzer may be used to regenerate H_2 and O_2 during the light portion (ref. 1). While the energy density for a H_2-O_2 system is large, the efficiency is considerably less than 100 percent due to the irreversibility of the O_2 electrode. Improved electrocatalysts are needed to minimize the

kinetic polarization losses resulting from this irreversibility for both fuel cell and electrolyzer conditions.

Recent GEO mission analysis indicated that a significant increase in the energy density is possible if the two-unit system is replaced with a single-unit system that uses passive means for water transfer and thermal control (ref.2). For this single-unit system, it is essential to develop new electrocatalysts for the O_2 electrode which are not only bifunctionally active and efficient but also chemically and electrochemically stable over the voltage range of about 0.7 to 1.5 V (i.e. the probable range for a practical single-unit regenerative H_2-O_2 fuel cell).

Perovskite and spinel oxides have been investigated for monofunctional electrocatalytic activity for either O_2 evolution or reduction. Studies of bifunctional electrocatalytic activity, however, are rare. The $NiCo_2O_4$ spinel is one of the more active electrocatalysts for O_2 evolution as illustrated in figure 1 (ref. 3). $NiCo_2O_4$ powder which can be made in high surface form is chemically stable in KOH and is a moderate electrical conductor. Electrolysis porous gas electrodes, fabricated from a mixture of $NiCo_2O_4$ powder and polytetrafloroethylene (PTFE) (i.e. PTFE-bonded), were reported to give over 1.3 A/cm^2 at 1.63 V in 5N KOH at 70 °C (ref. 4). Furthermore, this type of electrode was reported to be stable during O_2 evolution at 1 A/cm^2 with less than a 0.05 V increase in polarization after 3000 hr (ref. 5).

Very limited work has been done on electrocatalytic activity of spinel oxide catalysts for O_2 reduction. A polarization curve was reported for an "optimized" PTFE-bonded $NiCo_2O_4$ electrode which suggests that greater than 0.2 A/cm^2 can be obtained at 0.8 V. While very slow decomposition of the $NiCo_2O_4$ can be inferred from the reported corrosion currents, long time durability for the electrode was not established (ref. 6).

$NiCo_2O_4$ is reported to have certain characteristics other than bifunctional activity that make it useful as the electrocatalyst for a study of optimization of electrode fabrication techniques: ease of preparation as a high surface area powder; suitable preparation of a single phase by low temperature treatment of the precursors; and sufficient durability for proper electrode evaluation. Therefore, $NiCo_2O_4$ spinel was chosen as the electrocatalyst for a study of unsupported electrocatalysts fabricated into bifunctional, PTFE-bonded, porous gas fuel cell electrodes. The object of the present study was to measure its bifunctional activity and to observe what performance differences might result from different commercial electrode fabricators, using the same catalyst powder, held to similar specifications.

EXPERIMENTAL

Fabrication of Electrodes

High surface area $NiCo_2O_4$ powder was prepared by ELTECH Corp. using the coprecipitation method (ref. 7). Hydroxides were coprecipitated from dilute solutions of Co and Ni (2:1 ratio) chlorides by KOH. The gelatinous mixture was filtered and washed. The resulting residue was heated at 400 °C for 5 hr

in air to produce $NiCo_2O_4$ powder. This powder, which contains a wide range of particle or agglomerate sizes, was primarily $NiCo_2O_4$ spinel with some NiO present as an impurity (ref. 8). A surface measurement (BET) of this powder, using a Beta Scientific Automatic Surface Analyzer Model 4200, gave an area of 43 m^2/g.

PTFE-bonded, porous gas electrodes were fabricated by three commercial sources using the $NiCo_2O_4$ powder prepared by ELTECH Corp. While fabrication techniques are considered by the fabricators to be proprietary, some details are reportable. A catalyst-PTFE mixture was pressed onto a 100 mesh Au plated Ni screen and the resulting "green" electrode was heat treated. Electrode parameters are given in Table I. All electrodes contain essentially the same weight loadings of $NiCo_2O_4$. PTFE contents of either 15 or 25 percent of the $NiCo_2O_4$ were used. Electrodes 1 and 5 have a Gortex[1] PTFE backing at the gas side. This type of backing serves as a barrier to liquid electrolyte but not to gaseous O_2.

Electrochemical Apparatus and Measurements

A floating half-cell was used for all electrochemical measurements (ref. 9). A schematic of the cell is shown in figure 2. A working electrode (1.266 cm^2 of geometric area) was introduced into the cell with the catalyst side of the electrode touching the surface of the 31 percent KOH. Pt foil served as the counter electrode and a Hg/HgO electrode served as the reference electrode. The temperature coefficient for the Hg/HgO reference, shown in figure 3, was about -4.5×10^{-4} V/°C. Therefore, Hg/HgO reference potentials obtained at 25 and 80 °C correspond to reversible H_2 electrode potentials (RHE) of 0.926 and 0.902 V, respectively.[2] Gaseous O_2 was passed through a presaturator, maintained at the same temperature as the cell, and then into the cell. This presaturation minimizes H_2O loss and thus changes in KOH concentration during the test runs.

For most of the measurements, a potentiostat (EG&G Princeton Applied Research Model 173), with a plug-in unit (EG&G Model 276) was interfaced with a computer system (Apple IIe). A computer program (EG&G Electrochemistry Program Volume I) was used to drive and control the potentiostat. IR polarization values were determined by means of an IR instrument (Electrosynthesis Corp. Model 800) in conjunction with a 7 V Zener diode. Schematics are shown in figures 4(a) and 4(b). The IR instrument interrupts the run periodically for an interval of a few microseconds. The Zener diode limits the voltage rise of the potentiostat to 7 V during the interruption.

PTFE-bonded, porous gas electrodes often require preconditioning, prior to steady-state measurements, to minimize polarizations. Therefore each $NiCo_2O_4$ electrode was preconditioned at 80 °C by slowly increasing the anodic currents (at less than 2 V) until 1 A could be obtained. Usually, this time interval required less than 20 to 30 min. The anodic current was then decreased to about 0.1 A and held for about 1 hr. While holding at 0.1 A the height of the working electrode was adjusted relative to the KOH surface to minimize electrode and IR polarizations.

---

[1]Gortex is a trade name of W.L. Gore & Co.

[2]All potential values in this report will refer to RHE unless otherwise stated.

Steady-state, potential-current values were determined galvanostatically starting at the larger currents (e.g. 1 A). Each potential measurement was recorded with time for an interval of 3 to 6 min. As illustrated for electrode 5 in figures 5 (a) and (b), steady-state conditions were usually obtained after 10 to 30 sec, particularly for the larger currents. Even at the smaller currents (e.g. 0.001 A), less than 3 min was required to obtain steady-state conditions.

IR corrected potentials were obtained from plots of IR polarizations versus currents as illustrated in figure 6 for a typical run.

RESULTS

O_2 Evolution

O_2 evolution at nonaged PTFE-bonded $NiCo_2O_4$ electrodes. - At larger anodic currents, O_2 gas produced in the electrode pores may force some of the KOH electrolyte out of these pores (ref. 4). In addition, detachment of O_2 bubbles from the electrode surface becomes increasingly more difficult at these larger currents. As a consequence, the steady-state potentials (and IR polarizations) at larger currents become more erratic and difficult to measure. This is illustrated in figure 7 for a typical run at 0.6 A where the potential became erratic after only a few seconds. Therefore, data obtained at anodic currents above about 0.2 A were not recorded.

Electrode 5 (table I) was anodically preconditioned at 0.1 A but was not held at potentials more anodic than 1.5 V for an extended period of time (i.e. aged) prior to its being examined for O_2 evolution. Then, O_2 evolution data were obtained galvanostatically for this nonaged electrode. An IR corrected Tafel plot, obtained at 80 °C, is shown in figure 8. The Tafel slope for this nonaged electrode at the smaller current region (i.e. less than 0.060 A/cm^2) was about 0.045 V/decade. This value of 0.045 is in excellent agreement with the value of 0.047 reported for a PTFE-bonded $NiCo_2O_4$ electrode at 25 °C (ref. 10). Sufficient data were not obtained for the larger current region to determine its slope.

O_2 evolution at aged PTFE-bonded $NiCo_2O_4$. - Nonaged $NiCo_2O_4$ undergoes slow irreversible changes at more anodic potentials with accompanying changes in its electrocatalytic activity for O_2 evolution. The aging process was reported to be complete after about 2 hr if the electrode is maintained at potentials more anodic than 1.5V (ref. 11). It can be seen in figure 9 that the performance of the aged electrode is poorer than that of the nonaged electrode. However, the characteristics of the aged electrode will determine long-term performance of the catalyst in a practical energy storage system. Therefore, all $NiCo_2O_4$ electrodes were aged anodically at 1 A for about 6 to 7 hr.

After aging, steady-state, current-potential data were obtained galvanostatically for the 6 electrodes starting at the larger currents. The IR corrected Tafel data for each aged electrode could be fitted to 2 straight line regions: a slope of 0.12 V/decade was obtained for the larger currents and a slope of 0.060 V/decade was obtained for the smaller currents. A typical IR corrected Tafel plot (electrode 5) is shown in figure 9. For comparison, the corresponding Tafel data for nonaged electrode 5 are also shown in figure 9 as a dashed line.

The geometric exchange current density can be determined by extrapolation of the Tafel data to the thermodynamic potential of H_2O at 80 °C (i.e. 1.18 V). This extrapolated value can be calculated from the data using the following expression:

$$1.18 = A + (S)(\log i_o)$$

where A is the potential at 1 A/cm^2 in volts, S is the slope in V/decade, and i_o is the geometric exchange current density in A/cm^2. Estimating the "true" exchange current density for a porous gas electrode involves relating the total available surface area of the catalyst in the electrode to the electrode geometric surface area. The total surface area of the $NiCo_2O_4$ powder in the electrode can be estimated from the powder surface area (43 m^2/g), as determined by BET, and the quantity of powder used in the electrode. The "true" surface of the electrode can then be calculated by assuming 100 percent availability of the $NiCo_2O_4$ powder surface area. This assumption of 100 percent availability is supported by a BET measurement of electrode 1 after it had been used for electrochemical studies. For example, electrode 1 initially contained 0.027 g/cm^2 of $NiCo_2O_4$ powder corresponding to a value of about 1.2×10^4 cm^2 of "true" available surface area if 100 percent availability is assumed. A BET measurement of this electrode after aging gave a value of about 1.4×10^4 cm^2.

The Tafel results for each electrode are listed in Table II. For the 0.12 V/decade slope region, electrodes 1, 2, 3, and 4 gave essentially the same value for the potential at 0.1 A/cm^2 and, consequently, essentially the same geometric exchange current density for this region. Averaging the values for these 4 electrodes gave values of 1.466 V for the potential at 0.1 A/cm^2, 4.2×10^{-4} A/cm^2 for the geometric exchange current density and 3.9×10^{-8} A/cm^2 for the "true" exchange current density. If a maximum error of about 0.01 V is estimated for the potentials at 0.1 A/cm^2, the potentials for similar electrodes should range between 1.436 and 1.456 V. The corresponding calculated geometric exchange current densities for these potentials of 1.436 and 1.456 V are 3.4×10^{-4} and 5.5×10^{-4} A/cm^2, respectively. Electrodes 1, 2, 3, and 4 lay within this range. There were differences, however, in the fabrication processes for these 4 electrodes both in PTFE content and heat treatment. Consider electrodes 2 and 4; both had been fabricated by Electrochem Inc. with a 300 °C heat treatment, but with PTFE contents of 25 and 15 percent, respectively. Since both gave essentially the same Tafel data for the higher current region, PTFE contents within the range of 15 to 25 percent may not be a critical parameter for optimizing PTFE-bonded $NiCo_2O_4$ electrodes for O_2 evolution. Unlike that for electrodes 1, 2, 3, and 4, the geometric exchange current density for electrode 6 was almost a factor of 2 smaller than the estimated lower limit of 3.4×10^{-4} A/cm^2. Electrodes 4 and 6 were fabricated by Electrochem Inc. with the same PTFE content (15 percent) but were heat treated at 300 and 275 °C, respectively. A minimum heat treatment of 300 °C, therefore, is considered to be an important parameter for optimizing an electrode for O_2 evolution performance. Heating at 275 °C may not be sufficient to properly sinter the PTFE-$NiCo_2O_4$ mixture.

For the smaller current region (0.060 V/decade), electrodes 1, 2, 3, and 4 gave similar values for the potentials at 0.01 A/cm^2 and for the corresponding geometric exchange current densities. Averaging the results for these 4 electrodes gave values of 1.382 V for the potential at 0.01 A/cm^2, 4.8×10^{-6} A/cm^2 for the geometric exchange current density and 4.3×10^{-10} A/cm2 for the "true"

geometric exchange current density. If a maximum error of about 0.01 V is estimated for these potentials at 0.01 A/cm^2, the range for the geometric exchange current densities is between 2.9×10^{-6} and 6.3×10^{-6} A/cm^2. While the values for electrodes 1, 2, 3, and 4 lie close to this range, the value for the geometric exchange current density for electrode 6 is almost an order of magnitude smaller than the average of these 4 electrodes.

The O_2 evolution data for aged electrode 1 (obtained in the present study) is compared in figure 10 as a dashed line with data reported in the literature for aged, PTFE-bonded $NiCo_2O_4$ electrodes. Values for one electrode at 25 °C were taken from figure 1 of Botejue Nadesan (ref. 7). For this electrode, the "true" catalyst surface area, assuming 100 percent utilization of the $NiCo_2O_4$ powder surface area, was similar to that calculated for electrode 1 but its catalytic activity is less than that of electrode 1. The values for a second electrode at 84 °C were taken from figure 1 of Davidson (ref. 12). Its total catalyst surface area was estimated to be about one-half that of electrode 1. While complete details of the fabrication techniques (e.g. PTFE contents) for the Davidson electrode were not reported, its Tafel data for both current regions were similar to that obtained for electrode 1 of the present study particularly when the data are normalized to similar total catalyst surface areas.

Mechanisms for O_2 evolution at $NiCo_2O_4$. - Mechanisms have been proposed for the O_2 evolution process at oxide surfaces, but a definitive mechanism is still in question. For example, one proposed mechanism suggests that a higher valence oxide intermediate is formed at the $NiCo_2O_4$ spinal surface. This intermediate is subsequently decomposed to produce O_2 (ref. 13). More recently, molecular orbital calculations have been used to study O_2 evolution at the surface of a $SrFeO_3$ perovskite. For this oxide, the Fe species is forced into the +4 valence state if the O sites are filled. It was proposed that the reaction was initiated by an attack of OH^- at the Fe^{+4} species on a face site (ref.14). The first two steps for both of these mechanisms are similar in that an oxide intermediate is formed at the surface. The two mechanisms differ, however, in the subsequent formation of O_2 from the oxide intermediate. Mehandru's mechanism (ref. 14) involves the formation and then decomposition of a peroxide species while Rasiyah's mechanism (ref. 13) involves the decomposition of the oxide intermediate by means of a second metal species.

A series of reactions, which involves only a minor modification of Mehandru's mechanism, is presented here to account for the O_2 evolution processes occurring with slopes of 0.12 and 0.06 V/decade at aged $NiCo_2O_4$ surfaces. In this series, M represents a higher valence cation species (e.g. Co^{+3}) rather than Fe^{+4} as proposed by Mehandru for $SrFeO_3$.

M	+ OH^-	M-OH	+ e	(A)
M-OH	+ OH^-	$(M-O)^{-1}$	+ HOH	(B)
$(M-O)^{-1}$		M-O	+ e	(C)
M-O	+ OH^-	M-O-OH	+ e	(D)
M-O-OH	+ OH^-	M-O-O	+ HOH + e	(E)
M-O-O		M	+ O_2	(F)

Rasiyah reported a slope of about 0.04 V/decade for the smaller current region. A reaction similar to reaction (C) (given above) was proposed for the rate controlling step for this region (ref. 13). In the present study, a slope of about 0.045 V/decade was obtained for a nonaged $NiCo_2O_4$ electrode for

the smaller current region; but, after aging, the slope became 0.06. A more plausible explanation for the change from 0.045 to 0.06, therefore, involves aging of the $NiCo_2O_4$ by conversion of the metal species at the surface to higher valence states. This aging process will be discussed later in more detail.

After aging, all 6 aged $NiCo_2O_4$ electrodes gave slopes of 0.12 and 0.060 V/ decade. These values of 0.12 and 0.06 are in agreement with the hypothesis that reaction (A) is the rate-determining step for the larger current region and that reaction (B) is the rate-determining step for the smaller current region. For example, if a Langmuir condition (i.e. small absorption) is assumed, an anodic Tafel slope can be calculated from the number of electrons transferred using the following expression:

$$S_a = \frac{[RT]}{[F][b(\ell - k + n/v) - \ell]} \qquad (1)$$

where S_a is the anodic slope in V/decade, b is the beta symmetry factor (0.5), ℓ is the number of electrons which must be removed prior to the rate-determining step to permit the rate-determining step to occur once, k is the number of electrons which must be removed to permit the products of one occurrence of the rate-determining step to be transferred to the final state, n is the total number of electrons transferred in the over-all reaction, v is the stoichiometric number which is equal to the number of times that the rate-determining step occurs when the over-all reaction occurs once, and R, T and F have the usual significance (i.e. RT/F = 0.059 for 25 °C) (ref. 15). For the larger current region, a value of about 0.12 V/decade is calculated for the slope if reaction (A) is assumed to be the rate-determining step. For this calculation, the following values are used for reaction (A): $n = 4$, $\ell = 0$, $k = 3$, and $v = 1$. For the smaller current region, a slope of about 0.06 is calculated for the slope if reaction (B) is assumed to be the rate-determining step. For this calculation of the smaller current slope, the following values are used for reaction (B): $n = 4$, $\ell = -1$, $k = 3$ and $v = 1$.

An alternative type of mechanism has been proposed in an attempt to account for the observed change in slope from 0.12 to 0.06 for processes occurring at Pt catalysts. As the current decreases from the larger currents, the coverage changes from a Langmuir adsorption (i.e. small coverage) to Temkin adsorption (larger coverage). It has been proposed that for some electrochemical processes the coverage proceeds linearly with potential, thereby modifying the relation between the slope and the number of electrons transferred (refs. 16 and 17). As a consequence, the slope may change from 0.12 to 0.06 V/decade for the same 1 electron transfer step. If this type of mechanism is the controlling one for O_2 evolution at the $NiCo_2O_4$ surface, reaction (A) could predominate for both current regions with Temkin adsorption controlling for the smaller current region and Langmuir adsorption controlling for the larger current region. However, a recent study suggests that a change from Langmuir to Temkin adsorption does not contribute significantly to an observed change in slope. For example, this study indicated that the difference between steady-state, current-potential curves during the change from Langmuir to Temkin adsorption is relatively small owing to the dual effects of Temkin adsorption on the coverage and on the apparent rate constants (ref. 18). Therefore, the authors of the present study believe that this alternate type of mechanism does not contribute significantly to the observed change in slope for O_2 evolution at aged $NiCo_2O_4$ surfaces.

Anodic aging of the $NiCo_2O_4$ surface. - As discussed previously, the slope for the O_2 evolution process for the smaller current region changed from about 0.045 to 0.06 V/decade during anodic aging at 1 A for more than about 6 hr. During this aging process certain irreversible changes occurred at the $NiCo_2O_4$ surface.

This change in the surface composition during aging is supported by analyses reported for aged and nonaged $NiCo_2O_4$ electrodes. For example, analyses for Ni, Co, O and C, as determined by x-ray photoelectron spectroscopy (XPS), were reported by Haenen for surfaces of "freshly" prepared (i.e. nonaged) and for aged $NiCo_2O_4$ electrodes using $NiCo_2O_4$ powder prepared by decomposing Co and Ni (2:1) mixed nitrates at 300 and 400 °C (ref. 19) Carbon, present as a contaminant from the experimental system, was also included in the analyses. The reported analytical results were recalculated in the present paper for Ni, Co and O by excluding C. The stoichiometries of the $NiCo_2O_4$ surfaces for aged and nonaged electrodes were then calculated. For this calculation, an ideal $NiCo_2O_4$ spinel structure of $(Co + Ni)_3O_4$ is assumed. For the nonaged electrodes (300 and 400 °C), the stoichiometries indicated that O deficiencies were present for both electrode surfaces. The surface compositions for these 2 nonaged electrodes were then calculated by assuming the following: the total Co and Ni content was equal to 3; Co is oxidized more readily than Ni; and charge balance is maintained. Therefore, the surface compositions for the 2 nonaged $NiCo_2O_4$ electrodes can be expressed as follows:

(1) $(Ni^{+2})_{0.83}(Co^{+2})_{1.80}(Co^{+3})_{0.37}(O^{-2})_{3.16}$ ($NiCo_2O_4$ prepared at 300 °C)

(2) $(Ni^{+2})_{1.48}(Co^{+2})_{0.90}(Co^{+3})_{0.62}(O^{-2})_{3.33}$ ($NiCo_2O_4$ prepared at 400 °C)

Both of these nonaged electrodes have similar surface compositions: a large O deficiency is present; most (or all) of the Ni is present in the +2 valence state; and Co is present in both the +2 and +3 state.

For the aged electrode, analyses were reported only for the electrode which was fabricated using $NiCo_2O_4$ that was prepared at 300 °C (ref. 19). The surface stoichiometry was recalculated in the present study by excluding C. This calculation indicated that the O content had increased sufficiently during aging so that a stoichiometry of 4 can be assumed for the O content at the surface with a corresponding deficiency of cation species (Co + Ni). Therefore, the surface composition for this aged $NiCo_2O_4$ can be expressed as follows:

$(Ni^{+2})_{0.50}(Ni^{+3})_{0.18}(Co^{+3})_{2.16}(O^{-2})_{4.00}$ ($NiCo_2O_4$ prepared at 300 °C)

By comparing the compositions calculated for the surfaces of the above aged and nonaged electrodes, it is concluded that the aging process for the $NiCo_2O_4$ electrodes used in the present study is accompanied by the following:

(1) O is added to the surface thereby minimizing the large O deficiency that was present initially in the nonaged $NiCo_2O_4$.

(2) The Co deficiency, present initially in the nonaged electrode (where some of the Co sites are filled with Ni^{+2}), is minimized.

(3) Some of the Ni^{+2}, which was the principal Ni species at the nonaged $NiCo_2O_4$ surface, is oxidized to Ni^{+3}.

(4) Most (or all) of the Co species, present in the nonaged electrode as Co^{+2}, is oxidized to Co^{+3}.

O_2 Reduction

Stability of PTFE-bonded $NiCo_2O_4$ electrodes. - If $NiCo_2O_4$ is to be considered as a bifunctional catalyst in a single-unit energy storage system, the $NiCo_2O_4$ should have good stability between the voltage range of 0.7 and 1.5 V as well as good activity. The long time durability of $NiCo_2O_4$ has not been sufficiently established to date. For example, moderate stability, as indicated by corrosion current measurements, has been reported for $NiCo_2O_4$ at voltages more anodic than about 0.6 V (ref. 6). Another study, however, suggested that $NiCo_2O_4$ decomposes irreversibly below about 0.7 to 0.9 V (ref. 11). A third study also indicated that decomposition occurred for a $NiCo_2O_4$ coating formed on a oxidized Ni:2Co alloy, as indicated by a decrease in O_2 reduction current with time at potentials below about 0.6 V (ref. 20).

In the present study, all 6 aged $NiCo_2O_4$ electrodes showed electrode disintegration even at moderate cathodic currents. For example, solids were observed in the electrolyte at potentials below about 0.7 V. While some of the $NiCo_2O_4$ spinel in the electrode may be decomposing at these voltages, it appeared that most of the electrode disintegration was due to shedding of $NiCo_2O_4$ from the current collector.

O_2 reduction at PTFE-bonded $NiCo_2O_4$ electrodes. - While decomposition of $NiCo_2O_4$ occurs at lower potentials, its rates probably are sufficiently slow in the voltage range of interest to allow steady-state, current-potential data to be obtained. Atomic absorption spectrophotomer analysis supports this assumption. For example, analyses of the KOH solutions, after the electrodes had been used for the O_2 reduction studies, showed that the solutions contained less than 5 $\mu g/cm^3$ (the limit of detection) of both Ni and Co.

The 6 electrodes which were used previously for the O_2 evolution studies were cathodically preconditioned by holding at about -0.05 A for about 5 min. Current-potential data were then obtained galvanostatically starting at about -0.05 A and then reducing the current a few millivolts for each subsequent steady-state measurement. The Tafel results for O_2 reduction at the 6 electrodes are shown in figure 11. Poor O_2 mass transfer and poor electrode optimization for all 6 electrodes were evident as indicated by the short current range for which O_2 reduction data could be fitted to straight line regions. For example, the highest activity was obtained for electrode 5. The deviation from straight line regions for electrode 5 is shown more clearly in figure 12. Tafel data were obtained for electrode 5 only up to about -0.02 A/cm^2 after which the potential decreased rapidly with only small increases in current.

While O_2 reduction data for most of the $NiCo_2O_4$ electrodes were not obtained at currents less than about -0.0005 A/cm^2, two Tafel regions were assumed to be present for all 6 electrodes. For electrode 5, as illustrated

in figure 13, a slope of -0.06 V/decade was obtained for the current range of -0.001 to -0.010 A/cm^2. For the current range of -0.010 to -0.020 A/cm^2, the data for electrode 5 could be fitted to a straight line with a slope of -0.12 V/decade. Determining this Tafel slope was difficult since increased O_2 concentration polarization was occurring. For electrode 6 as illustrated in figure 14, a slope of about -0.12 V/decade was obtained for the current range of -0.0008 to -0.004 A/cm^2. Presumably, a slope of -0.06 would also have been observed if smaller currents had been used. Therefore, slopes of -0.06 and -0.12 V/decade were assumed for all 6 electrodes as given in Table III.

As seen in table III, more scatter in the data was observed for the reduction of O_2 in the region of -0.12 volt/decade than for the corresponding O_2 evolution process. For example, the calculated geometric exchange current densities for the O_2 reduction process ranged between 9×10^{-7} and 2.8×10^{-5} A/cm^2 for the 6 electrodes for this region. This scatter may be related to the quantity of PTFE used and its effect on the electrode structure. The effect of PTFE content would be expected to be more significant for the O_2 reduction process since O_2 is transported to the reaction sites by moving through the PTFE fibers.

The geometric exchange densities for the -0.12 region for electrodes 1, 2, and 5 are larger than those for electrodes 3, 4, and 6. Electrodes, 1, 2, and 5 had PTFE contents of 25 percent while electrodes 3, 4, and 6 all contained 15 percent PTFE. This effect of increased activity with increased PTFE content is also illustrated by comparing electrodes 2 and 4, both of which were obtained from the same commercial source. Both electrodes were sintered at the same temperature, 300 °C, but had PTFE contents of 25 and 15 percent respectively. The geometric exchange current density for electrode 2 was almost twice that of electrode 4. It was concluded, therefore, that a PTFE content of 25 percent (or greater) may be preferred for optimizing PTFE-bonded $NiCo_2O_4$ porous gas electrodes for O_2 reduction catalytic activity.

The data obtained in the present study for electrode 5 is compared in figure 15 with data reported for O_2 reduction at $NiCo_2O_4$. For one study, one datum point was reported for O_2 reduction at 0.9 V at 80 °C. For this electrode, $NiCo_2O_4$ powder of 80 m^2/g was used, but the sintering conditions were not given (ref. 21). The current at 0.9 V is in reasonable agreement with that obtained in the present study for electrode 5. Electrode 5 was also compared with data reported for an "optimized" electrode (ref. 22). While only a few data points were reported for this electrode, slopes of about -0.06 and -0.12 V/decade can be assumed for these data along with an initiation of O_2 concentration polarization at larger currents, in reasonable agreement with the present study. The currents obtained for this optimized electrode were about 5 times larger than those found in the present study for electrode 5. The "optimization" technique, however, was not reported.

Mechanisms for O_2 reduction at $NiCo_2O_4$. - A slope of about -0.06 V/decade was reported for a $NiCo_2O_4$ electrode at 80 °C, (ref. 23) which is in good agreement with that found in the present study for the smaller current region. Conflicting results, however, were reported for the O_2 reduction process by Trasatti (ref. 3 p. 243). For example, Trasatti reported that one study obtained 2 regions with slopes of -0.06 and -0.12 V/decade and corresponding exchange current densities of 3.2×10^{-13} and 6.3×10^{-10} A/cm^2,

respectively. These values are in fair agreement with the values obtained in the present study. Two other studies reported by Trasatti gave conflicting results. One study suggested slopes of -0.06 and -0.20 V/decade while the second study suggested 3 slopes of -0.06, -0.12 and -0.20 V/decade.

While O_2 reduction proceeds by means of a peroxide mechanism for several oxides (e.g. NiO), this is not the case for O_2 reduction at $NiCo_2O_4$ spinel surfaces. Instead, it has been reported that the process proceeds primarily by means of a 4 electron process to form OH^- for the potential range between 0.7 and 0.8 V as indicated by the rotating ring-disk study (ref. 20) At these potentials, the formation of peroxide was found to produce less than 10 percent of the total current. But at 0.3 V, where the rate of decomposition of $NiCo_2O_4$ spinel to produce NiO is much faster, the rate of peroxide formation is essentially equal to the direct 4 electron process.

A mechanism for the initial steps in O_2 reduction at a $NiCo_2O_4$ surface has been reported which is similar to the reverse process for O_2 evolution (ref. 24). A series of reactions which involves only a minor modification of Tarasevich's mechanism (ref. 24) is proposed to account for the two slope regions observed in the present study. In this series, M probably represents a lower valence metal species (e.g. Co^{+2}). Breaking the peroxide bond is difficult. As a consequence, several steps are involved for the continuing reduction of peroxide to form OH^-. Steps for the continued reduction of the peroxide are combined and are shown below as reaction (K).

$$M + O_2 \longrightarrow M\text{-}O_2 \quad (G)$$

$$M\text{-}O_2 + e \longrightarrow (M\text{-}O_2)^- \quad (H)$$

$$(M\text{-}O_2)^- + HOH \longrightarrow M\text{-}O_2H + OH^- \quad (I)$$

$$M\text{-}O_2H + e \longrightarrow (M\text{-}O_2H)^- \quad (J)$$

$$(M\text{-}O_2H)^- + 2e + HOH \longrightarrow M + 3OH^- \quad (K)$$

The values of -0.12 and -0.06 V/decade obtained in the present study for the slopes are in agreement with the hypothesis that reaction (H) is the rate-determining step for the larger current region and that reaction (I) is the rate-determining step for the small current region. For these calculations, the expression is as follows:

$$S_c = \frac{(-RT)}{(F)[k + (1 - b)(\ell - k + n/v)]}$$

where S_c is the cathodic slope, k is the number of electrons which must be added prior to the rate-determining step to permit the rate-determining step to occur once, ℓ is the number of electrons that must be added to permit the products formed by one occurrence of the rate-determining step to be transferred to the final state, b is the beta symmetry factor (0.5), n is the total number of electrons transferred in the over-all reaction and v is the stoichiometric number (ref. 15). For the larger current region, a value of about -0.12 V/decade is calculated for the slope if reaction (H) is assumed to be the rate-determining step. For this calculation, the following values are used for reaction (H): $n = 4$, $k = 0$, $\ell = -3$, and $v = 1$. For the smaller current region, a value if -0.06 is calculated for the slope using the following values for reaction (I): $n = 4$, $k = 1$, $\ell = -3$, and $v = 1$.

As discussed previously, the authors of the present study believe that an alternate mechanism involving Langmuir and Temkin adsorption is not a major

contributor to changing the slope from -0.12 to -0.06 V/decade for the smaller current region.

SUMMARY

$NiCo_2O_4$ spinel was chosen as the catalyst for a study of its bifunctional electrocatalytic activity for the O_2 electrode and of techniques of fabricating it into PTFE-bonded, porous gas electrodes. For this study, 6 electrodes were fabricated by 3 commercial sources by means of proprietary techniques using varying PTFE contents and sintering temperatures.

The following may be stated regarding the O_2 evolution studies:

1. An irreversible reaction occurs at the $NiCo_2O_4$ surface if the electrode is held at more anodic potentials (i.e. aged at greater than about 1.5 V) for a few hours. This change is due to the oxidation of Ni and Co surface sites to form stable, higher oxidation states.

2. Good catalytic activity for O_2 evolution is obtained for aged electrodes at current densities up to about 0.2 A/cm^2. Removal of O_2 bubbles at current densities above 0.2 A/cm^2, however, becomes increasingly more difficult.

3. Tafel data, obtained for all 6 aged electrodes, are similar in that 2 slopes are obtained for each electrode. A slope of 0.12 V/decade is obtained for the larger current region while a slope of 0.06 is obtained for the smaller current region.

4. Four of the electrodes gave essentially the same calculated values for the geometric exchange current densities, particularly for the 0.12 slope region. The PTFE content for these 4 electrodes was either 15 or 25 percent of the $NiCo_2O_4$, while the sintering conditions ranged between 300 and 340 °C. One electrode which was sintered at only 275 °C gave a smaller value for the exchange current density (i.e. by a factor of 3).

Therefore, within the range of 15 to 25 percent, the PTFE content is not a critical parameter for optimizing aged PTFE-bonded $NiCo_2O_4$ electrodes for improved activity for O_2 evolution. Furthermore, sintering temperatures between 300 and 340 °C may be adequate, but that heating at 275 °C may not be sufficient to properly sinter the PTFE-$NiCo_2O_4$ mixture.

The following may be stated regarding the O_2 reduction studies:

1. Electrode disintegration was observed during cathodic runs. It is still not clear whether this disintegration was due primarily to a physical shedding of the $NiCo_2O_4$ from the current collector screen or to electrochemical decomposition of the spinel to form oxides of Ni and Co.

2. Transport polarization of O_2 to the $NiCo_2O_4$ surface became prohibitive for all of the electrodes at current densities greater than about -0.02 A/cm^2.

3. Two Tafel regions can be assumed for all 6 Tafel curves. A slope of -0.12 V/decade was assumed for the moderate current density region and a slope of -0.06 was assumed for the smaller current density region.

4. The catalytic activity for O_2 reduction at these electrodes was much smaller than that which was obtained for the corresponding O_2 evolution processes as indicated by the respective exchange current densities. Furthermore, the activity for O_2 reduction in the present study was about a factor of 5 smaller than that which was estimated from data reported by others for an "optimized" $NiCo_2O_4$ electrode.

Therefore, a PTFE content of 25 percent (or greater) appears to be preferable for sintering PTFE-bonded $NiCo_2O_4$ porous gas electrodes for improved O_2 reduction activity.

REFERENCES

1. Baraona, C.R.; and Sheibley, D.W.: Status of Space Station Power System. Space Electrochemical Research and Technology (SERT), NASA CP-2484, 1987, pp. 1-8.

2. Van Dine, L.; Gonzalez-Sanabria, O.; and Levy, A.: Regenerative Fuel Cell Study for Satellites in GEO Orbit. AIAA Paper 87-9200, Aug. 1987. (NASA TM-89914).

3. Trasatti, S.; and Lodi, G.: Oxygen and Chlorine Evolution at Conductive Metallic Oxide Anodes. Electrodes of Conductive Metallic Oxides, Part B, S. Trasatti, ed., Elsevier Scientific Publishing Co., 1981, pp. 521-626.

4. Tseung, A.C.C.; Jasem, S.; and Mahmood, M.N.: Oxygen Evolution on Porous Semiconducting Oxide Electrodes. Proceedings of the Symposium on Industrial Water Electrolysis, S. Srinivasan, F.J. Salzano, and A.R. Landgrebe, eds., Electrochemical Society, 1978, pp. 161-168.

5. Tseung, A.C.C., et al.: Optimization of Gas Evolving Teflon Bonded Electrodes. Hydrogen as an Energy Vector, A.S. Strub and G. Imarisio, eds., D. Reidel Publishing Co., Boston, 1980, pp. 240-246.

6. King, W.J.; and Tseung, A.C.C.: The Reduction of Oxygen on Nickel-Cobalt Oxides. I. The Influence of Composition and Preparation Method on the Activity of Nickel-Cobalt Oxides. Electrochim. Acta, vol. 19, no. 8, Aug. 1974, pp. 485-491.

7. Nadesan, J.C. B.; and Tseung, A.C.C.: Effect of Mesh Size on the Performance of Teflon Bonded Oxygen-Evolving Electrodes. J. Appl. Electrochem., vol. 15, no. 6, Nov. 1985, pp. 961-967.

8. Singer, J., et al.: Phase Purity of $NiCo_2O_4$, a Catalyst Candidate for Electrolysis of Water. NASA TM-100239, 1987.

9. Giner, J.; and Smith, S.: A Simple Method for Measuring Polarization of Hydrophobic Gas Diffusion Electrodes. Electrochem. Tech., vol. 5, no. 1-2, Jan.-Feb. 1967, pp. 59-61.

10. Jasem, S.M.; and Tseung, A.C.C.: A Potentiostatic Pulse Study of Oxygen Evolution on Teflon-Bonded Nickel-Cobalt Oxide Electrodes. J. Electrochem. Soc., vol. 126, no. 8, Aug. 1979, pp. 1353-1360.

11. Haenen, J.; Visscher, W.; and Barendrecht, E.: Characterization of $NiCo_2O_4$ Electrodes for O_2 Evolution. Part III. Aging Phenomena of $NiCo_2O_4$ Electrodes. J. Electroanal. Chem., vol. 208, 1986, pp. 323-341.

12. Davidson, C.R.; Kissel, G.; and Srinivasan, S.: Electrode Kinetics of the Oxygen Evolution Reaction at $NiCo_2O_4$ from 30% KOH. Dependence on Temperature. J. Electroanal. Chem., vol. 132, 1982, pp. 129-135.

13. Rasiyah, P.; and Tseung, A.C.C.: A Mechanistic Study of Oxygen Evolution on $NiCo_2O_4$. II. Electrochemical Kinetics. J. Electrochem. Soc., vol. 130, no. 12, Dec. 1983, pp. 2384-2386.

14. Mehandru, S.P.; and Anderson, A.B.: Oxygen Evolution on a $SrFeO_3$ Anode. Mechanistic Considerations from Molecular Orbital Theory. To be published.

15. Fraser, G.H.; and Barradas, R.G.: A Simplified Calculation of Tafel Slopes for Successive Electrochemical Reactions. J. Electrochem. Soc., vol. 112, no. 4, Apr. 1965, pp. 462-464.

16. Sepa, D.B.; Vojnovic, M.V.; and Damjanovic, A.: Kinetics and Mechanisms of O_2 Reduction at Pt in Alkaline Solutions. Electrochim. Acta, vol. 25, no. 11, Nov. 1980, pp. 1491-1496.

17. Sepa, D.B.; Vojnovic, M.V.; and Damjanovic, A.: Reaction Intermediates as a Controlling Factor in the Kinetics and Mechanism of Oxygen Reduction at Platinum Electrodes. Electrochim. Acta, vol. 26, no. 6, June 1981, pp. 781-793.

18. Saraby-Reintjes, A.: Electrocatalysis Under Temkin Adsorption Conditions. J. Chem. Soc. Faraday Trans. 1, vol. 83, pt. 2, 1987, pp. 271-279.

19. Haenen, J.; Visscher, W.; and Barendrecht, E.: Characterization of $NiCo_2O_4$ Electrodes for O_2 Evolution. Part II. Non-Electrochemical Characterization of $NiCo_2O_4$ Electrodes. J. Electroanal. Chem., vol. 208, 1986, pp. 297-321.

20. Bagotzky, V.S.; Shumilova, N.A.; and Khrushcheva, E.I.: Electrochemical Oxygen Reduction on Oxide Catalysts. Electrochim. Acta, vol. 21, no. 11, Nov. 1976, pp. 919-924.

21. Martin, R.E.: Advanced Technology Light Weight Fuel Cell Program. (FCR-1657, United Technologies Corp.; NASA Contract NAS3-21257) NASA CR-159807, 1980, p. 40.

22. Vassie, P.R.; and Tseung, A.C.C.: A Study of Gas Evolution in Teflon Bonded Porous Electrodes. II. Factors Affecting the Mechanical Strength. Electrochem. Acta, vol. 20, no. 10, Oct. 1975, pp. 763-765.

23. Singh, G.; Miles, M.H.; and Srinivasan, S.: Mixed Oxides as Oxygen Electrodes. Electrocatalysis on Non-Metallic Surfaces, NBS SP-455, A.D. Franklin, ed., National Bureau of Standards, 1975, pp. 289-296.

24. Tarasevich, M.R.; and Efremov, B.N.: Properties of Spinel-Type Oxide Electrodes. Electrodes of Conductive Metallic Oxides, Part B, S. Trasatti, ed., Elsevier Scientific Publishing Co., 1981, pp. 221-259.

TABLE I. - PTFE-BONDED, $NiCo_2O_4$ POROUS GAS ELECTRODES

Electrode number	Fabrication source	$NiCo_2O_4$ content, Mg/cm^2	PTFE content, percent of $NiCo_2O_4$	Heating temperature, °C
1	Prototech Corp.	27	25	340
2	Electrochem Inc.	25	25	300
3	Electrochem Inc.	25	15	325
4	Electrochem Inc.	25	15	300
5	Electromedia Corp.	25	25	340
6	Electrochem Inc.	25	15	275

TABLE II. - POTENTIALS AND EXCHANGE CURRENT DENSITIES FOR O_2 EVOLUTION USING AGED, PTFE-BONDED $NiCo_2O_4$ POROUS GAS ELECTRODES

(a) Region of 0.12 V/decade slope (larger currents)

Electrode number	Potential at 0.1 A/cm^2, V	Exchange current density	
		Geometric, A/cm^2	"True", A/cm^2
1	1.467	4.1×10^{-4}	3.5×10^{-8}
2	1.464	4.3	4.0
3	1.463	4.4	4.1
4	1.466	4.1	3.8
5	1.498	2.2	2.0
6	1.516	1.6	1.5

(b) Region of 0.06 V/decade slope (smaller currents)

Electrode number	Potential at 0.01 A/cm^2, V	Exchange current density	
		Geometric, A/cm^2	"True", A/cm^2
1	1.363	8.9×10^{-6}	7.7×10^{-10}
2	1.390	3.2×10^{-6}	3.0×10^{-10}
3	1.387	3.5×10^{-6}	3.3×10^{-10}
4	1.387	3.5×10^{-6}	3.3×10^{-10}
5	1.422	9.3×10^{-7}	8.7×10^{-11}
6	1.436	5.4×10^{-7}	5.0×10^{-11}

TABLE III. - POTENTIALS AND EXCHANGE CURRENT DENSITIES FOR O_2 REDUCTION USING PTFE-BONDED, $NiCo_2O_4$ POROUS GAS ELECTRODES

(a) Region of -0.12 V/decade slope (moderate currents)

Electrode number	Potential at 0.01 A/cm^2, V	Exchange current		Current density range, A/cm^2
		Geometric, A/cm^2	"True", A/cm^2	
5	0.873	2.8×10^{-5}	2.6×10^{-9}	0.010 to 0.020
1	[a].803	7.2×10^{-6}	6.2×10^{-10}	.003 to .008
2	[a].753	2.8×10^{-6}	2.6×10^{-10}	.003 to .006
6	[a].730	1.8×10^{-6}	1.7×10^{-10}	.0008 to .004
4	[a].710	1.2×10^{-6}	1.1×10^{-10}	.001 to .003
3	[a,b].692	9×10^{-7}	8×10^{-11}	.002 to .003

(b) Region of -0.06 V/decade slope (smaller currents)

Electrode number	Potential at 0.001 A/cm^2, V	Exchange current		Current density range, A/cm^2
		Geometric, A/cm^2	"True", A/cm^2	
5	0.934	7.9×10^{-8}	7.3×10^{-12}	0.001 to 0.010
1	.891	1.5×10^{-8}	1.4×10^{-12}	.0004 to .003
2	.844	2.5×10^{-9}	2.3×10^{-13}	.0004 to .003
6	-----	---------	---------	----------
4	-----	---------	---------	----------
3	[b].798	4×10^{-10}	4×10^{-14}	<0.002

[a]Extrapolated.
[b]Estimated.

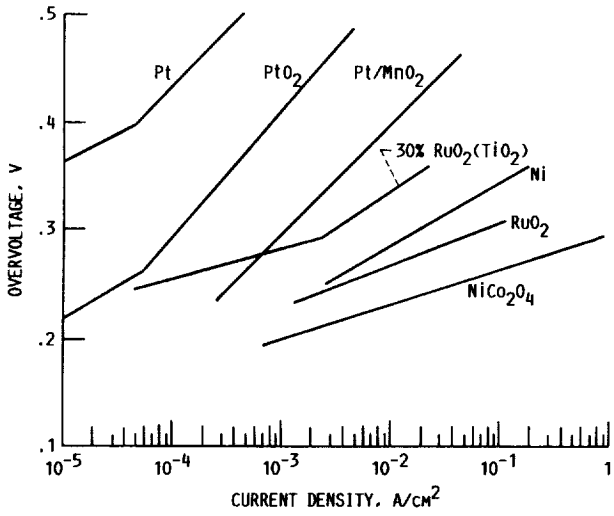

FIGURE 1. - OVERPOTENTIAL-CURRENT DENSITY CURVES FOR O_2 EVOLUTION ON VARIOUS OXIDES FROM ALKALINE SOLUTIONS.

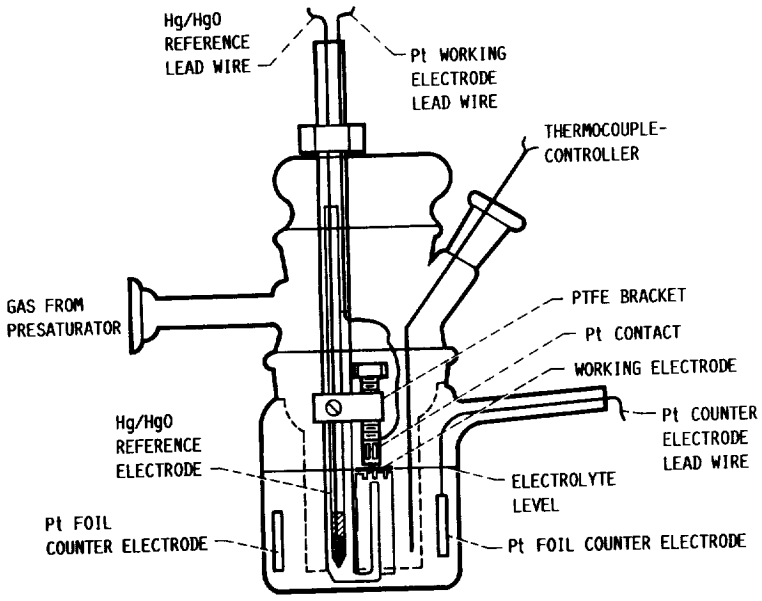

FIGURE 2. - SCHEMATIC OF FLOATING HALF-CELL.

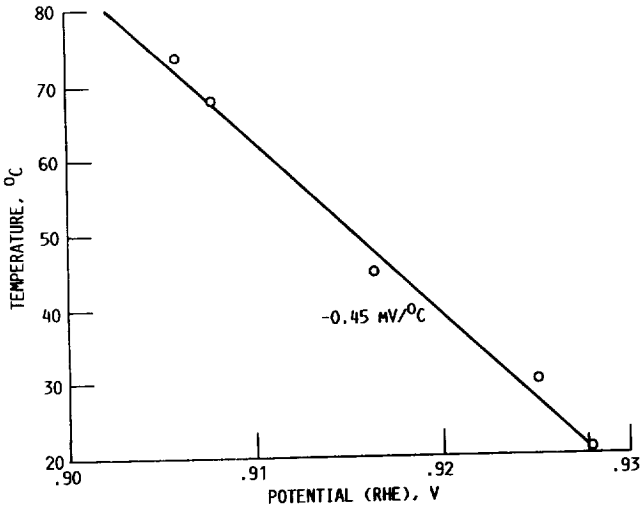

FIGURE 3. - Hg/HgO REFERENCE ELECTRODE POTENTIAL COMPARED WITH DYNAMIC H_2 ELECTRODE POTENTIAL (1 ATM O_2, 31% KOH).

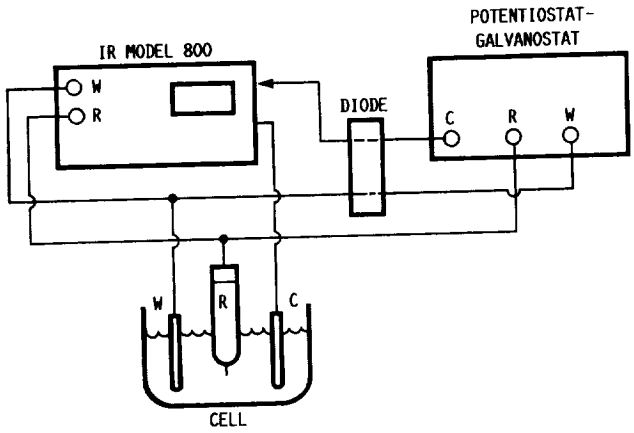

(a) SCHEMATIC FOR CONNECTION OF CELL AND EQUIPMENT TO ELECTRO-SYNTHESIS CORPORATION MODEL 800 IR INSTRUMENT.

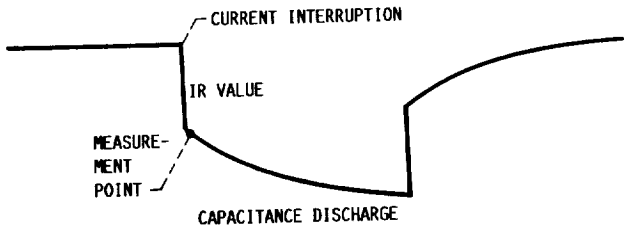

(b) SCHEMATIC OF TYPICAL IR WAVEFORM FOR WORKING ELECTRODE.

FIGURE 4. - IR POLARIZATION DETERMINATION.

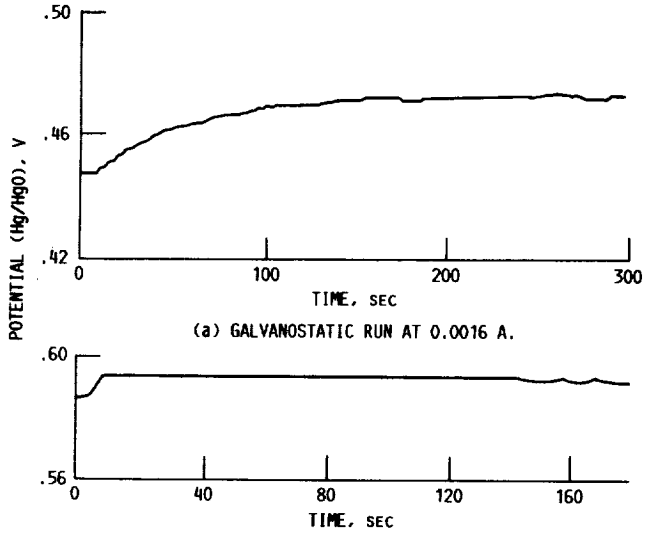

(a) GALVANOSTATIC RUN AT 0.0016 A.

(b) GALVANOSTATIC RUN AT 0.050 A.

FIGURE 5. - POTENTIAL VERSUS TIME FOR O_2 EVOLUTION RUNS FOR $NiCo_2O_4$ ELECTRODE 5 (1 ATM O_2, 80 ^{o}C, 31% KOH).

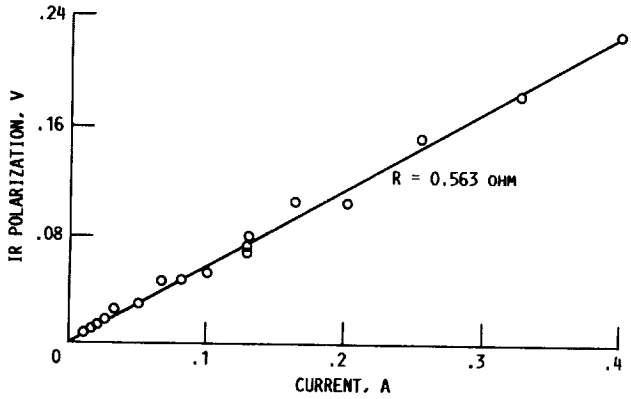

FIGURE 6. - IR POLARIZATION VERSUS CURRENT FOR STEADY-STATE GALVANOSTATIC O_2 EVOLUTION RUN FOR AGED $NiCo_2O_4$ ELECTRODE 2 (1 ATM O_2, 80 ^{o}C, 31% KOH).

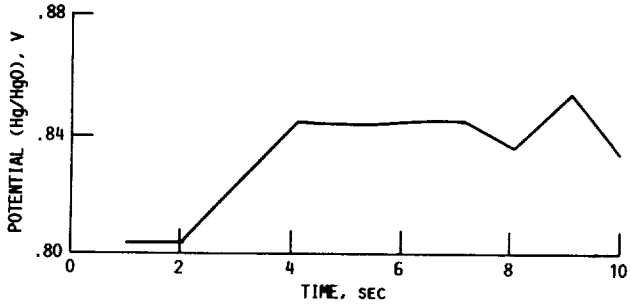

FIGURE 7. - POTENTIAL VERSUS TIME FOR GALVANOSTATIC O_2 EVOLUTION RUN AT 0.6 A FOR TYPICAL $NiCo_2O_4$ ELECTRODE (1 ATM O_2, 80 ^{o}C, 31% KOH).

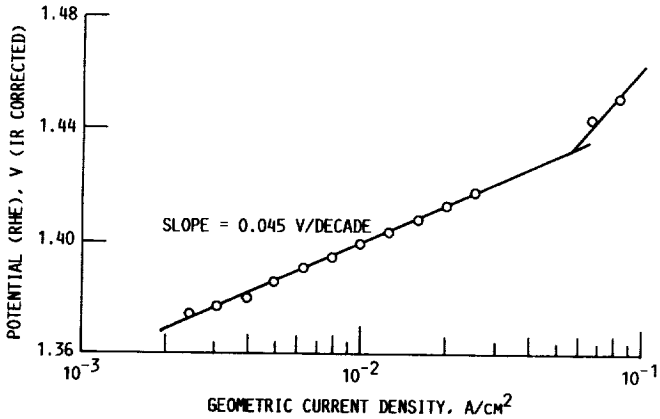

FIGURE 8. - TAFEL PLOT FOR STEADY-STATE GALVANOSTATIC O_2 EVOLUTION RUN FOR NONAGED $NiCo_2O_4$ ELECTRODE 5 (1 ATM O_2, 80 ^{o}C, 31% KOH).

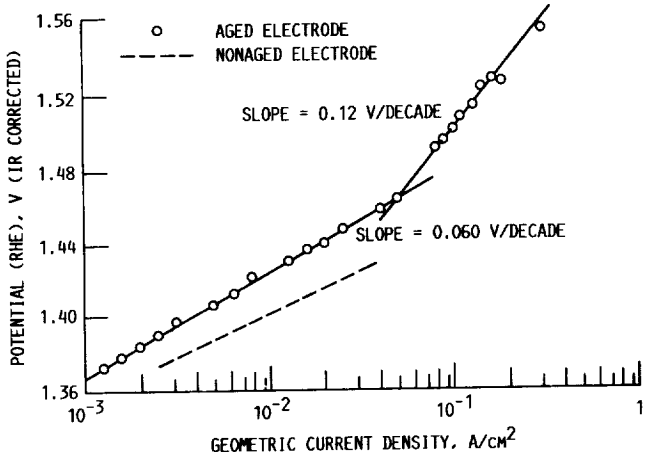

FIGURE 9. - TAFEL PLOT FOR STEADY-STATE GALVANOSTATIC O_2 EVOLUTION RUN FOR $NiCo_2O_4$ ELECTRODE 5 (1 ATM O_2, 80 ^oC, 31% KOH).

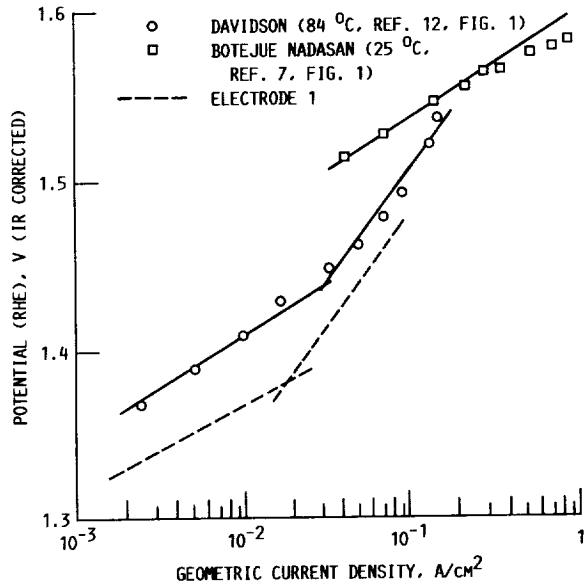

FIGURE 10. - COMPARISON OF TAFEL O_2 EVOLUTION DATA FOR ELECTRODE 1 WITH THAT OF DAVIDSON AND BOTEJUE NADASAN.

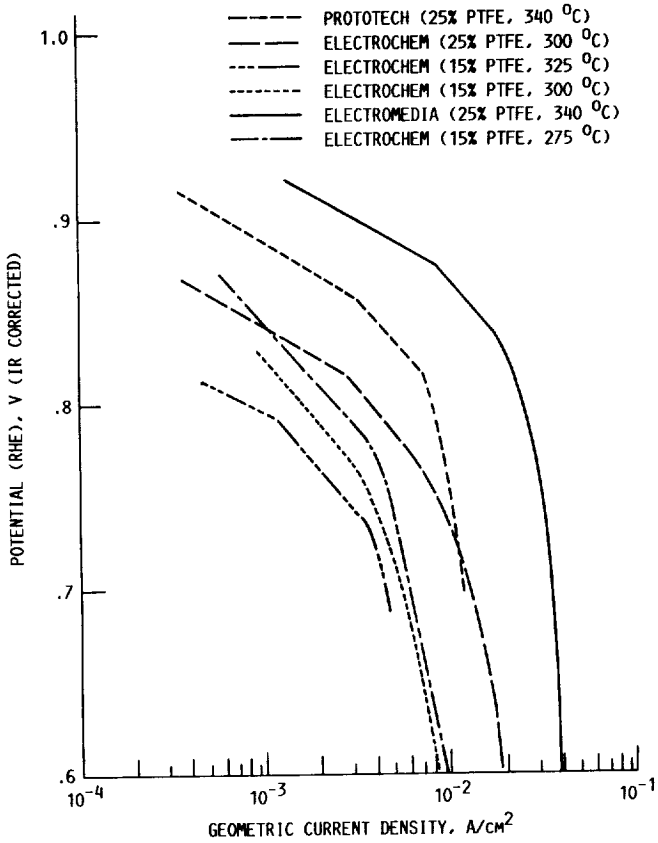

FIGURE 11. - TAFEL PLOT FOR STEADY-STATE GALVANOSTATIC O_2 REDUCTION OF $NiCo_2O_4$ ELECTRODES (1 ATM O_2, 80 ^oC, 31% KOH).

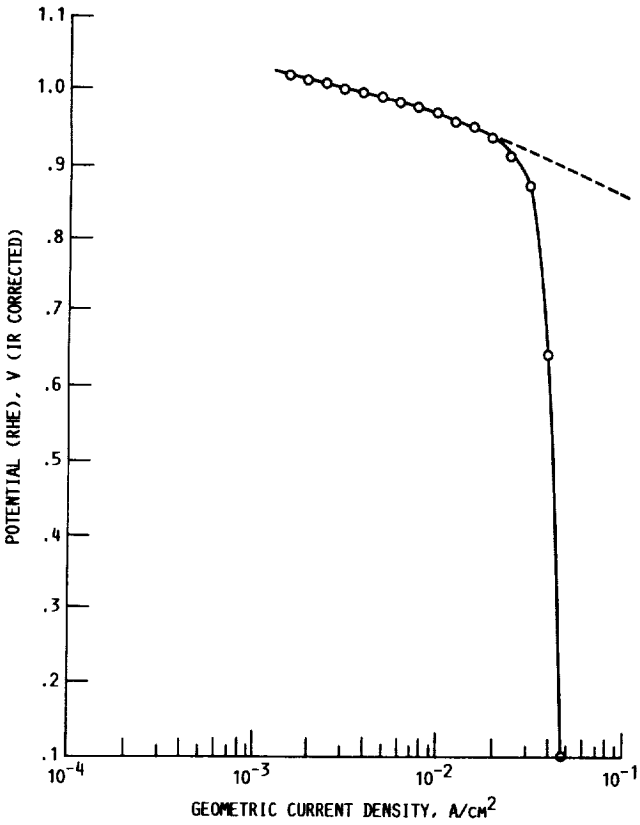

FIGURE 12. - TAFEL PLOT FOR STEADY-STATE GALVANOSTATIC O_2 REDUCTION AT AGED $NiCo_2O_4$ ELECTRODE 5 (1 ATM O_2, 80 ^oC, 31% KOH).

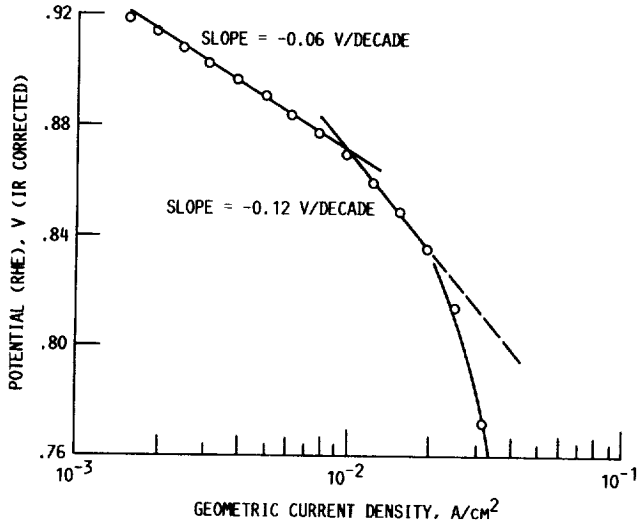

FIGURE 13. - TAFEL PLOT FOR STEADY-STATE GALVANOSTATIC O_2 REDUCTION AT AGED $NiCo_2O_4$ ELECTRODE 5 (1 ATM O_2, 80 ^oC, 31% KOH).

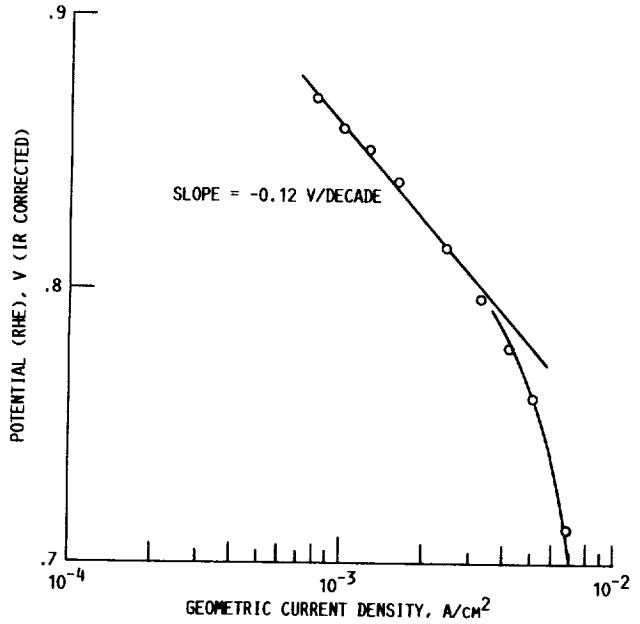

FIGURE 14. - TAFEL PLOT FOR STEADY-STATE GALVANOSTATIC O_2 REDUCTION AT AGED $NiCo_2O_4$ ELECTRODE 6 (1 ATM O_2, 80 ^oC, 31% KOH).

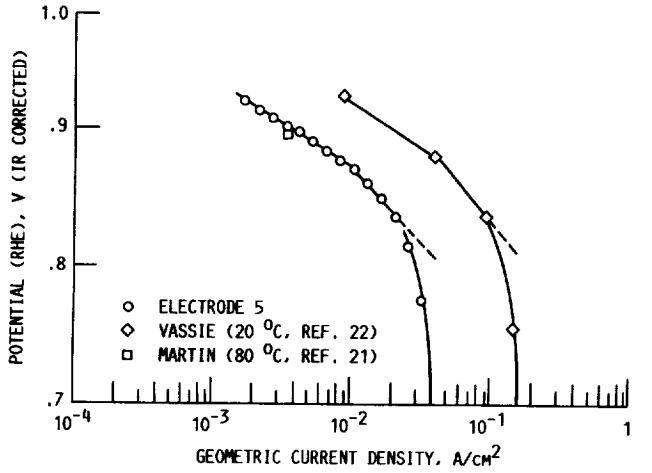

FIGURE 15. - COMPARISON OF TAFEL O_2 REDUCTION DATA FOR ELECTRODE 5 WITH THAT OF REPORTED DATA.

NASA
National Aeronautics and Space Administration

Report Documentation Page

1. Report No.	2. Government Accession No.	3. Recipient's Catalog No.
NASA TM-100947		

4. Title and Subtitle	5. Report Date
Oxygen Electrode Bifunctional Electrocatalyst $NiCo_2O_4$ Spinel	September 1988
	6. Performing Organization Code

7. Author(s)	8. Performing Organization Report No.
William L. Fielder and Joseph Singer	E-4238
	10. Work Unit No.
	506-41-21

9. Performing Organization Name and Address	11. Contract or Grant No.
National Aeronautics and Space Administration Lewis Research Center Cleveland, Ohio 44135-3191	
	13. Type of Report and Period Covered
	Technical Memorandum
12. Sponsoring Agency Name and Address	14. Sponsoring Agency Code
National Aeronautics and Space Administration Washington, D.C. 20546-0001	

15. Supplementary Notes

16. Abstract

A significant increase in energy density may be possible if a two-unit alkaline regenerative H_2-O_2 fuel cell is replaced with a single-unit system that uses passive means for H_2O transfer and thermal control. For this single-unit system, new electrocatalysts for the O_2 electrode will be required which are not only bifunctionally active but also chemically and electrochemically stable between the voltage range of about 0.7 and 1.5 V. $NiCo_2O_4$ spinel is reported to have certain characteristics that make it useful for a study of electrode fabrication techniques. High surface area $NiCo_2O_4$ powder was fabricated into unsupported, bifunctional, PTFE-bonded, porous gas fuel cell electrodes by commercial sources using varying PTFE contents and sintering temperatures. The object of the present study was to measure the bifunctional activities of these electrodes and to observe what performance differences might result from different commercial electrode fabricators. O_2 evolution and O_2 reduction data were obtained at 80 °C (31 percent KOH). An irreversible reaction (i.e. aging) occurred during O_2 evolution at potentials greater than about 1.5 V. Anodic Tafel slopes of 0.06 and 0.12 V/decade were obtained for the aged electrodes. Within the range of 15 to 25 percent, the PTFE content was not a critical parameter for optimizing the electrode for O_2 evolution activity. Sintering temperatures between 300 and 340 °C may be adequate but heating at 275 °C may not be sufficient to properly sinter the PTFE-$NiCo_2O_4$ mixture. Electrode disintegration was observed during O_2 reduction. Transport of O_2 to the $NiCo_2O_4$ surface became prohibitive at greater than about -0.02 A/cm^2. Cathodic Tafel slopes of -0.06 and -0.12 V/decade were assumed for the O_2 reduction process. A PTFE content of 25 percent (or greater) appears to be preferable for sintering the PTFE-$NiCo_2O_4$ mixture.

17. Key Words (Suggested by Author(s))	18. Distribution Statement
$NiCo_2O_4$ Bifunctional electrocatalyst O_2 electrode	Unclassified – Unlimited Subject Category 44

19. Security Classif. (of this report)	20. Security Classif. (of this page)	21. No of pages	22. Price*
Unclassified	Unclassified	22	A02

*For sale by the National Technical Information Service, Springfield, Virginia 22161

National Aeronautics and
Space Administration

Lewis Research Center
Cleveland, Ohio 44135

FOURTH CLASS MAIL

ADDRESS CORRECTION REQUESTED

Official Business
Penalty for Private Use $300

Postage and Fees Paid
National Aeronautics and
Space Administration
NASA 451

NASA